

PERFORMANCE ANALYSIS OF CROSS-BAND ADAPTATION FOR SUBBAND ACOUSTIC ECHO CANCELLATION

Yekutiel Avargel and Israel Cohen

Department of Electrical Engineering, Technion - Israel Institute of Technology
Technion City, Haifa 32000, Israel
{kutiav@tx, icohen@ee}.technion.ac.il

ABSTRACT

In this paper, we analyze the performance of cross-band adaptation in the short-time Fourier transform (STFT) domain for the application of acoustic echo cancellation. The band-to-band filters and the cross-band filters considered in each frequency-band are all estimated by adaptive filters, which are updated by the LMS algorithm. We derive explicit expressions for the transient and steady-state mean-square error (MSE) in subbands for both correlated and white Gaussian processes. The theoretical analysis is supported by experimental results.

1. INTRODUCTION

Subband acoustic echo cancellation systems generally require adaptive cross-band filters for the identification of time-varying echo path [1]. Recently, we investigated the influence of cross-band filters on the performance of an acoustic echo canceller implemented in the STFT domain, and analyzed the steady-state mean-square error (MSE) in subbands [2]. We derived explicit relations between the cross-band filters in the STFT domain and the impulse response in the time domain. It has been shown that in order to capture most of the energy of the STFT representation of the time domain impulse response, relatively few cross-band filters need to be considered.

In this paper, we analyze the convergence of a direct adaptive algorithm used for the adaptation of the cross-band filters in the STFT domain. The band-to-band filters and the cross-band filters considered in a given frequency-band are all estimated by adaptive filters, which are updated by the LMS algorithm. Explicit expressions for the transient and steady-state MSE in subbands are derived for both correlated and white Gaussian processes. The number of cross-band filters used for the echo canceller in each frequency-band is generally lower than the number of filters needed for the STFT representation of the unknown echo path. We therefore employ the performance analysis of the deficient length LMS algorithm which was recently

presented in [3]. Experimental results are provided, which support our theoretical analysis and demonstrate the transient and steady-state MSE performances of the direct adaptation algorithm.

2. PROBLEM FORMULATION

An acoustic echo canceller operating in the STFT domain is depicted in Fig. 1. The microphone signal $y(n)$ can be written as $y(n) = d(n) + \xi(n)$, where $d(n)$ is the echo signal and $\xi(n)$ is the near-end signal. Applying the STFT to $y(n)$, we have in the time-frequency domain

$$y_{p,k} = d_{p,k} + \xi_{p,k}, \quad (1)$$

where p is the frame index ($p = 0, 1, \dots$) and k is the frequency-band index ($k = 0, 1, \dots, N-1$). $d_{p,k}$ can be written as [2]

$$d_{p,k} = \sum_{k'=0}^{N-1} \sum_{p'=0}^{N_h-1} x_{p-p',k'} h_{p',k,k'}, \quad (2)$$

where $h_{p',k,k'}$ depends on both the echo path impulse response $h(n)$ and the STFT analysis/synthesis parameters, and N_h is its length (with respect to index p'). That is, for a given frequency-band index k , the signal $d_{p,k}$ is obtained by convolving the signal $x_{p,k'}$ in each frequency-band k' with the corresponding filter $h_{p,k,k'}$ and then summing over all the outputs. We refer to $h_{p,k,k'}$ for $k = k'$ as a band-to-band filter and for $k \neq k'$ as a cross-band filter. It has been shown [2] that in order to capture most of the energy of the STFT representation of $h(n)$, relatively few cross-band filters need to be considered. Our objective is to adapt those cross-band filters in the STFT domain in order to produce an echo estimate.

3. DIRECT ADAPTATION ALGORITHM

In this section, we present a direct adaptation algorithm (first introduced in [1]), in which each of the cross-band filters used for the echo canceller is estimated by using

This research was supported by the Israel Science Foundation (grant no. 1085/05).

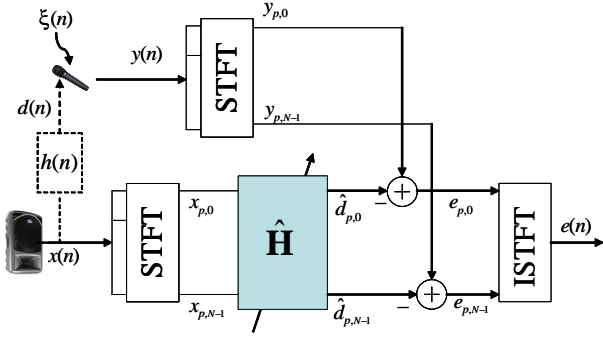


Figure 1: Acoustic echo cancellation system in the STFT domain. The echo path impulse response $h(n)$ is modeled by the block $\hat{\mathbf{H}}$ in the STFT domain.

an adaptive filter. Let $\hat{h}_{p',k,k'}(p)$ be an adaptive filter of length N_h that attempts to estimate the cross-band filter $h_{p',k,k'}$ at frame index p , and let $\hat{d}_{p,k}$ be the resulting estimate of $d_{p,k}$ using only $2K$ adaptive filters around the frequency-band k , where $2K + 1 \leq N$, i.e.,

$$\hat{d}_{p,k} = \sum_{k'=k-K}^{k+K} \sum_{p'=0}^{N_h-1} x_{p-p',k'} \hat{h}_{p',k,k'}(p), \quad (3)$$

when we recall that due to the periodicity of the frequency-bands the summation index k' satisfies $k' = k' \bmod N$. Let $\mathbf{h}_{k,k'} = [h_{0,k,k'} \cdots h_{N_h-1,k,k'}]^T$ denote a cross-band filter from frequency-band k' to frequency-band k and let $\mathbf{X}_k(p) = [x_{p,k} \ x_{p-1,k} \ \cdots \ x_{p-N_h+1,k}]^T$. Then, using (1) and (2), $y_{p,k}$ can be rewritten as

$$y_{p,k} = \bar{\mathbf{x}}_k^T(p) \tilde{\mathbf{h}}_k + \xi_{p,k}, \quad (4)$$

where $\bar{\mathbf{x}}_k(p) = [\mathbf{X}_0^T(p) \ \cdots \ \mathbf{X}_{N-1}^T(p)]^T$ and $\tilde{\mathbf{h}}_k = [\mathbf{h}_{k,0}^T \ \cdots \ \mathbf{h}_{k,N-1}^T]^T$ are the column-stack concatenations of $\{\mathbf{X}_{k'}(p)\}_{k'=0}^{N-1}$ and $\{\mathbf{h}_{k,k'}\}_{k'=0}^{N-1}$, respectively. Let $\hat{\mathbf{h}}_{k,k'}(p) = [\hat{h}_{0,k,k'}(p) \ \cdots \ \hat{h}_{N_h-1,k,k'}(p)]^T$ denote an adaptive cross-band filter from frequency-band k to frequency-band k' . Then the estimated echo signal in (3) can be rewritten as

$$\hat{d}_{p,k} = \mathbf{x}_k^T(p) \hat{\mathbf{h}}_k(p), \quad (5)$$

where $\mathbf{x}_k(p)$ and $\hat{\mathbf{h}}_k(p)$ are the column-stack concatenations of $\{\mathbf{X}_{k'}(p)\}_{k'=k-K}^{k+K}$ and $\{\hat{\mathbf{h}}_{k,k'}(p)\}_{k'=k-K}^{k+K}$, respectively. The coefficients of the $2K + 1$ adaptive cross-band filters are then updated using the LMS algorithm:

$$\hat{\mathbf{h}}_k(p+1) = \hat{\mathbf{h}}_k(p) + \mu e_{p,k} \mathbf{x}_k^*(p) \quad (6)$$

where

$$e_{p,k} = y_{p,k} - \hat{d}_{p,k} \quad (7)$$

is the error signal (see Fig. 1), μ is the step-size and $*$ denotes complex conjugation. Observe that we attempt to estimate the unknown system in the STFT domain represented by a vector of length NN_h ($\tilde{\mathbf{h}}_k$), by using a deficient length vector $\hat{\mathbf{h}}_k(p)$ with only $(2K + 1)N_h$ coefficients. Let us write $\tilde{\mathbf{h}}_k$ and $\bar{\mathbf{x}}_k(p)$, respectively, as $\tilde{\mathbf{h}}_k = [\mathbf{h}_k^T \ \bar{\mathbf{h}}_k^T]^T$, $\bar{\mathbf{x}}_k(p) = [\mathbf{x}_k^T(p) \ \bar{\mathbf{x}}_k^T(p)]^T$ where \mathbf{h}_k , $\bar{\mathbf{h}}_k$ and $\bar{\mathbf{x}}_k(p)$ are the column-stack concatenations of $\{\mathbf{h}_{k,k'}\}_{k'=k-K}^{k+K}$, $\{\mathbf{h}_{k,k'}\}_{k' \in \mathcal{L}}$ and $\{\mathbf{X}_{k'}(p)\}_{k' \in \mathcal{L}}$, respectively, where $\mathcal{L} = \{k' | k' \in [0, N-1] \text{ and } k' \notin [k-K, k+K]\}$. Then, by substituting (4) and (5) into (7), the error signal can be written as

$$e_{p,k} = \bar{\mathbf{x}}_k^T(p) \bar{\mathbf{h}}_k - \mathbf{x}_k^T(p) \mathbf{g}_k(p) + \xi_{p,k}, \quad (8)$$

where $\mathbf{g}_k(p) = \hat{\mathbf{h}}_k(p) - \mathbf{h}_k$ represents the misalignment vector. Substituting (8) into (6), the LMS update equation can be expressed as

$$\begin{aligned} \mathbf{g}_k(p+1) &= [\mathbf{I} - \mu \mathbf{x}_k^*(p) \mathbf{x}_k^T(p)] \mathbf{g}_k(p) \\ &\quad + \mu [\bar{\mathbf{x}}_k^T(p) \bar{\mathbf{h}}_k] \mathbf{x}_k^*(p) + \mu \xi_{p,k} \mathbf{x}_k^*(p). \end{aligned} \quad (9)$$

4. MSE PERFORMANCE ANALYSIS

We proceed with the mean-square analysis of the adaptive algorithm assuming that $x_{p,k}$ is a zero-mean correlated Gaussian complex signal with variance σ_x^2 , and that $\xi_{p,k}$ is a zero-mean white complex signal with variance σ_ξ^2 that is uncorrelated with $x_{p,k}$. We also use the common independence assumption that $\mathbf{x}_k(p)$ is independent of $\hat{\mathbf{h}}_k(p)$ [4].

4.1. Transient Performance

The MSE is defined by

$$\epsilon_k(p) = E \left\{ |e_{p,k}|^2 \right\}, \quad (10)$$

Let $\mathbf{R}_k = E \{ \mathbf{x}_k(p) \mathbf{x}_k^H(p) \}$ and $\bar{\mathbf{R}}_k = E \{ \bar{\mathbf{x}}_k(p) \bar{\mathbf{x}}_k^H(p) \}$ be the autocorrelation matrices of $\mathbf{x}_k(p)$ and $\bar{\mathbf{x}}_k(p)$, respectively. Then, by substituting (8) into (10), the MSE can be expressed as

$$\begin{aligned} \epsilon_k(p) &= \sigma_\xi^2 + \bar{\mathbf{h}}_k^T \bar{\mathbf{R}}_k \bar{\mathbf{h}}_k^* - 2 \operatorname{Re} \{ \mathbf{f}_k^H E \{ \mathbf{g}_k(p) \} \} \\ &\quad + E \{ \mathbf{g}_k^T(p) \mathbf{R}_k \mathbf{g}_k^*(p) \} \end{aligned} \quad (11)$$

where $\mathbf{f}_k = \bar{\mathbf{h}}_k^T E \{ \bar{\mathbf{x}}_k(p) \mathbf{x}_k^*(p) \}$, the operator $tr(\cdot)$ denotes the trace of a matrix and H denotes conjugation transpose. Now, since \mathbf{R}_k is Hermitian matrix it can be decomposed into $\mathbf{R}_k = \mathbf{Q}_k \mathbf{\Lambda}_k \mathbf{Q}_k^H$, where $\mathbf{\Lambda}_k = \text{diag}(\lambda_k^1, \dots, \lambda_k^{(2K+1)N_h})$ is the diagonal eigenvalue matrix, λ_k^i is the i -th eigenvalue of \mathbf{R}_k , and \mathbf{Q}_k is a unitary matrix whose columns are the eigenvectors of \mathbf{R}_k . By decomposing \mathbf{R}_k in (11), the MSE can be rewritten as

$$\begin{aligned} \epsilon_k(p) &= \sigma_\xi^2 + \bar{\mathbf{h}}_k^T \bar{\mathbf{R}}_k \bar{\mathbf{h}}_k^* - 2 \text{Re} \{ \mathbf{f}_k^H E \{ \mathbf{g}_k(p) \} \} \\ &\quad + \boldsymbol{\lambda}_k^T \mathbf{z}_k(p), \end{aligned} \quad (12)$$

where $\boldsymbol{\lambda}_k = \text{diag}(\mathbf{\Lambda}_k)$ is a vector whose components are the diagonal elements of $\mathbf{\Lambda}_k$ and $\mathbf{z}_k(p) = \text{diag}(\mathbf{Q}_k^H E \{ \mathbf{g}_k^*(p) \mathbf{g}_k^T(p) \} \mathbf{Q}_k)$. To proceed with the analysis, we need to find recursive formulas for $E \{ \mathbf{g}_k(p) \}$ and $\mathbf{z}_k(p)$. By taking expectation in (9) and using the independence assumption we get

$$E \{ \mathbf{g}_k(p+1) \} = [\mathbf{I} - \mu \mathbf{R}_k^*] E \{ \mathbf{g}_k(p) \} + \mu \mathbf{f}_k. \quad (13)$$

Furthermore, substituting (9) into the expression for $\mathbf{z}_k(p)$ and using the fourth-order moment factoring theorem for zero-mean complex Gaussian samples, we obtain the following recursive formula for $\mathbf{z}_k(p)$:

$$\mathbf{z}_k(p+1) = \mathbf{A}_k \mathbf{z}_k(p) + \mathbf{b}_k(p) + \mu^2 \mathbf{c}_k + \mu^2 \sigma_\xi^2 \boldsymbol{\lambda}_k \quad (14)$$

where $\mathbf{A}_k = \mathbf{I} - 2\mu \mathbf{\Lambda}_k + \mu^2 \mathbf{\Lambda}_k^2 + \mu^2 \boldsymbol{\lambda}_k \boldsymbol{\lambda}_k^T$, $\mathbf{b}_k(p) = 2\mu \text{Re} \{ \mathbf{F}_k \mathbf{Q}_k^H E \{ \mathbf{g}_k^*(p) \} \}$ and $\mathbf{c}_k = \text{diag}(\mathbf{Q}_k^H \mathbf{C}_k \mathbf{Q}_k)$, where \mathbf{F}_k is a diagonal matrix whose diagonal contains the elements of the vector $\hat{\mathbf{f}}_k = \mathbf{Q}_k^T \mathbf{f}_k$ and $\mathbf{u}_k(p) = \text{diag}(\mathbf{Q}_k^H \mathbf{U}_k(p) \mathbf{Q}_k)$. The matrices $\mathbf{U}_k(p)$ and \mathbf{C}_k are given by

$$\begin{aligned} \mathbf{U}_k(p) &= E \{ [\bar{\mathbf{x}}_k^T(p) \bar{\mathbf{h}}_k] \mathbf{x}_k(p) \mathbf{x}_k^H(p) \mathbf{z}_k^*(p) \mathbf{x}_k^H(p) \} \\ \mathbf{C}_k &= E \{ |\bar{\mathbf{x}}_k^T(p) \bar{\mathbf{h}}_k|^2 \mathbf{x}_k(p) \mathbf{x}_k^H(p) \}, \end{aligned} \quad (15)$$

where by defining $\tilde{\mathbf{R}}_k = E \{ \bar{\mathbf{x}}_k(p) \mathbf{x}_k^H(p) \}$, the (n, m) -th term of $\mathbf{U}_k(p)$ and \mathbf{C}_k can be written, respectively, as $(\mathbf{U}_k(p))_{n,m} = E \{ \mathbf{g}_k^H(p) \} \left[(\mathbf{R}_k)_{n,m} \tilde{\mathbf{R}}_k^T + (\mathbf{R}_k)_{n,:}^T \left(\tilde{\mathbf{R}}_k \right)_{:,m}^T \right] \bar{\mathbf{h}}$ and $(\mathbf{C}_k)_{n,m} = \bar{\mathbf{h}}^T \left[(\mathbf{R}_k)_{n,m} \bar{\mathbf{R}}_k + \left(\tilde{\mathbf{R}}_k \right)_{:,m} \left(\tilde{\mathbf{R}}_k^* \right)_{:,n}^T \right] \bar{\mathbf{h}}^*$, where $(\cdot)_{n,:}$ and $(\cdot)_{:,n}$ denote the n -th row and the n -th column of a matrix, respectively. Equations (12)-(15) represent the MSE behavior in the k -th frequency-band using a direct cross-band filters' adaptation.

4.2. Steady-State Performance

To examine the steady-state solution of (12), we first need to find the steady-state solutions of (13) and (14). It can be verified that equation (13) is convergent if μ satisfies

$$0 < \mu < \frac{2}{tr(\mathbf{R}_k^*)} = \frac{2}{tr(\mathbf{R}_k)} \quad (16)$$

and its steady-state solution is

$$E \{ \mathbf{g}_k(\infty) \} = (\mathbf{R}_k^*)^{-1} \mathbf{f}_k, \quad (17)$$

that is, $E \{ \hat{\mathbf{h}}_k(\infty) \} = \mathbf{h}_k + (\mathbf{R}_k^*)^{-1} \mathbf{f}_k$. It indicates that each of the adaptive cross-band filters does not converge in the mean to the true unknown cross-band filter and it suffers from a bias quantified by $(\mathbf{R}_k^*)^{-1} \mathbf{f}_k$. This bias, however, reduces to zero whenever $2K+1 = N$ (i.e., all the cross-band filters are estimated) or $x_{p,k}$ is white, which in both cases $\mathbf{f}_k = 0$. Substituting (17) for $\mathbf{g}_k(p)$ in (11) we find the minimum MSE (MMSE) obtainable in the k -th frequency-band:

$$\epsilon_k^{\min} = \sigma_\xi^2 + \bar{\mathbf{h}}_k^T \bar{\mathbf{R}}_k \bar{\mathbf{h}}_k^* - \hat{\mathbf{f}}_k^T \mathbf{\Lambda}_k^{-1} \hat{\mathbf{f}}_k^* \quad (18)$$

We proceed with deriving the steady-state solution of (14). Observe that $\mathbf{b}_k(p)$ in (14) is bounded whenever μ satisfies (16). As a result, equation (14) is convergent if and only if the eigenvalues of \mathbf{A}_k are all within the unit circle. Following the theoretical analysis in [5] we find that this condition results in

$$0 < \mu < \frac{1}{tr(\mathbf{R}_k)} \triangleq \mu_{\max}. \quad (19)$$

It is clear that condition (16) is dominated by (19), therefore the mean-square convergence of this algorithm is guaranteed if μ satisfies (19). The steady-state solution of (14) is given by

$$\mathbf{z}_k(\infty) = [\mathbf{I} - \mathbf{A}_k]^{-1} [\mathbf{b}_k(\infty) + \mu^2 \mathbf{c}_k + \mu^2 \sigma_\xi^2 \boldsymbol{\lambda}_k], \quad (20)$$

where $\mathbf{b}_k(\infty)$ can be easily computed using (15) and (17). Observe that by substituting (17) into (12), the steady-state MSE can be written as

$$\epsilon_k(\infty) = \epsilon_k^{\min} + \epsilon_k^{ex}(\infty), \quad (21)$$

where $\epsilon_k^{ex}(\infty) = \boldsymbol{\lambda}_k^T \mathbf{z}_k(\infty) - \hat{\mathbf{f}}_k^T \mathbf{\Lambda}_k^{-1} \hat{\mathbf{f}}_k^*$ is the steady-state excess MSE and ϵ_k^{\min} is defined in (18). Using the matrix inverse lemma to solve (20), we obtain after some manipulations

$$\epsilon_k^{ex}(\infty) = \frac{\sum_{i=1}^{(2K+1)N_h} \frac{\mu q_k^i}{2 - \mu \lambda_k^i} + \sum_{i=1}^{(2K+1)N_h} \frac{\mu \lambda_k^i \epsilon_k^{\min}}{2 - \mu \lambda_k^i}}{1 - \sum_{i=1}^{(2K+1)N_h} \frac{\mu \lambda_k^i}{2 - \mu \lambda_k^i}}, \quad (22)$$

where q_k^i is the i -th element of the vector $\mathbf{q}_k = \mathbf{c}_k - 2 \operatorname{Re} \{ \mathbf{u}_k(\infty) \} + \left[2 \hat{\mathbf{f}}_k^T \boldsymbol{\Lambda}_k^{-1} \hat{\mathbf{f}}_k^* - \bar{\mathbf{h}}_k^T \bar{\mathbf{R}}_k \bar{\mathbf{h}}_k^* \right] \boldsymbol{\lambda}_k + \operatorname{diag}(\hat{\mathbf{f}}_k \hat{\mathbf{f}}_k^H)$. Equations (21), (18) and (22) provide an explicit expression for the steady-state MSE achieved in each frequency-band using a direct adaptation for the cross-band filters. Note that for small step-size values, (22) can be written as

$$\epsilon_k^{ex}(\infty) \cong \frac{\mu}{2} \sum_{i=1}^{(2K+1)N_h} q_k^i + \frac{\mu}{2} \sum_{i=1}^{(2K+1)N_h} \lambda_k^i \epsilon_k^{\min}. \quad (23)$$

That is, the excess MSE is mainly influenced by both the fluctuations of the adaptive filters coefficients around the optimal values and the bias in those coefficients, caused by the deficient number of adaptive cross-band filters used in the algorithm. Note that when the input signal $x_{p,k}$ is white we have $\mathbf{q}_k = 0$, leading to simplified expressions for the steady-state MSE

$$\epsilon_k^{ex}(\infty)_{white} = \frac{\mu \sigma_x^2 (2K+1) N_h}{2 - \mu \sigma_x^2 [(2K+1) N_h + 1]} \epsilon_{k_{white}}^{\min}, \quad (24)$$

where $\epsilon_{k_{white}}^{\min} = \sigma_\xi^2 + \sigma_x^2 \|\bar{\mathbf{h}}_k\|^2$, and $\epsilon_k(\infty)_{white} = \epsilon_{k_{white}}^{\min} + \epsilon_k^{ex}(\infty)_{white}$.

5. SIMULATIONS RESULTS AND DISCUSSION

Simulations results verify the theoretical results derived in this paper. A sampling rate of 16 kHz was used. An impulse response $h(n)$ was measured in an office which exhibits a reverberation time (the time for the reverberant sound energy to drop by 60 dB from its original value) of about 300 ms. The STFT was applied to the desired signals by using a Hamming synthesis window of length $N = 256$ (16 ms) with 50% overlap ($L = 128$), and a corresponding minimum energy analysis window which satisfies the completeness condition [6]. The STFT of the far-end signal $x_{p,k}$ and the STFT of the near-end signal $\xi_{p,k}$ are both zero-mean white Gaussian processes with variances $\sigma_x^2 = 1$ and $\sigma_\xi^2 = 0.001$, respectively. We chose $K = 2$ (i.e., 4 adaptive cross-band filters), and used a large step-size $\mu = 0.006$ ($\approx 0.5\mu_{\max}$) and a small one $\mu = 0.0012$ ($\approx 0.1\mu_{\max}$). Fig. 2 shows the MSE curves for the frequency-band $k = 1$ that obtained from simulations (by averaging over 1000 independent runs) and from the theoretical expression in (12) (similar results are obtained for the other frequency-bands). It can be seen that the theoretical analysis accurately describes both the transient and steady-state performance of the direct adaptation algorithm. Generally, as the step-size increases, the theoretical MSE curves are less accurate in predicting the algorithm performance since the independence assumption

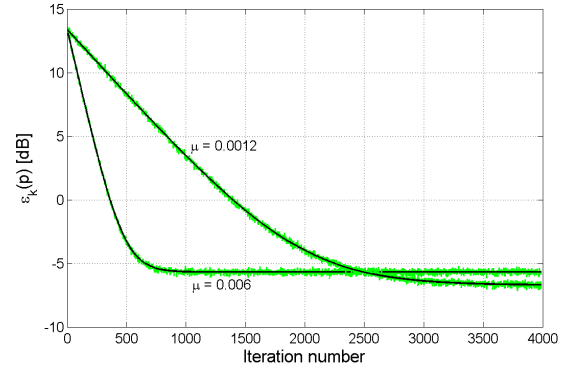


Figure 2: Comparison of simulation (light) and theoretical (dark) MSE curves for white Gaussian signals, obtained using a large step-size $\mu = 0.006$ and a small step-size $\mu = 0.0012$.

used in this paper is valid only for small step-size values. As expected from (24), as we decrease the step-size, lower steady-state MSE is achieved; however, the algorithm then suffers from slow convergence rate. Note that the analysis presented here is performed under the assumption of a uniform step-size for each adaptive cross-band filter. Performance may be further improved by incorporating different step-size values for each filter (e.g., matching the step-size to the signal energy at the input of each adaptive cross-band filter).

6. REFERENCES

- [1] A. Gilloire and M. Vetterli, "Adaptive filtering in subbands with critical sampling: Analysis, experiments, and application to acoustic echo cancellation," *IEEE Trans. Signal Process.*, vol. 40, no. 8, pp. 1862–1875, Aug. 1992.
- [2] Y. Avargel and I. Cohen, "Acoustic echo cancellation in the short-time Fourier transform domain with cross-band filtering," *submitted to IEEE Trans. Audio, Speech, Language Process.*
- [3] K. Mayyas, "Performance analysis of the deficient length LMS adaptive algorithm," *IEEE Trans. Signal Process.*, vol. 53, no. 8, pp. 2727–2734, Aug. 2005.
- [4] L. L. Horowitz and K. D. Senne, "Performance advantage of complex LMS for controlling narrow-band adaptive arrays," *IEEE Trans. Acoust., Speech, Signal Process.*, vol. ASSP-29, no. 3, pp. 722–736, Jun. 1981.
- [5] A. Feuer and E. Weinstein, "Convergence analysis of LMS filters with uncorrelated Gaussian data," *IEEE Trans. Acoust., Speech, Signal Process.*, vol. ASSP-33, no. 1, pp. 222–230, Feb. 1985.
- [6] J. Wexler and S. Raz, "Discrete Gabor expansions," *Signal Process.*, vol. 21, pp. 207–220, Nov. 1990.